

VERIFYING CONSISTENCY OF EFFECTIVE-VISCOSITY AND PRESSURE-LOSS DATA FOR DESIGNING FOAM PROPORTIONING SYSTEMS

Bogdan Z. Dlugogorski¹, Ted H. Schaefer^{1,2} and Eric M. Kennedy¹

¹Process Safety and Environment Protection Research Group

School of Engineering

The University of Newcastle

Callaghan, NSW 2308, AUSTRALIA

Phone: +61 2 4921 6176, Fax: +61 2 4921 6920

Email: Bogdan.Dlugogorski@newcastle.edu.au

²3M Specialty Materials Laboratory

Dunheved Circuit, St Marys, NSW 2760, AUSTRALIA

ABSTRACT

Aspirating and compressed-air foam systems often incorporate proportioners designed to draw sufficient rate of foam concentrate into the flowing stream of water. The selection of proportioner's piping follows from the engineering correlations linking the pressure loss with the flow rate of a concentrate, for specified temperature (usually 20 °C) and pipe size. Unfortunately, reports exist that such correlations may be inaccurate, resulting in the design of underperforming suppression systems. To illustrate the problem, we introduce two correlations, sourced from industry and developed for the same foam concentrate, that describe effective viscosity (μ_{eff}) and pressure loss as functions of flow rate and pipe diameter. We then present a methodology to verify the internal consistency of each data set. This methodology includes replotting the curves of the effective viscosity vs the nominal shear rate at the wall ($32Q/(\pi D^3)$) and also replotting the pressure loss in terms of the stress rate at the wall (τ_w) vs the nominal shear rate at the wall. In the laminar regime, for time-independent fluids with no slip at the wall (which is the behaviour displayed by foam concentrates), consistent data sets are characterised by a single curve of μ_{eff} vs $32Q/(\pi D^3)$, and a single curve of τ_w vs $32Q/(\pi D^3)$ in the laminar regime. We demonstrate that neither of the data sets shows internal consistency, and suggest possible errors in data processing that led to the observed discrepancies. Finally, we correct the original data to produce the engineering correlations, which are internally consistent and which are characterised by realistic rheology.

KEYWORDS ATC-AFFF, AR-AFFF, alcohol tolerant concentrates, alcohol resistant foams, class B foams, rheology of foam concentrates, flow and pressure losses of non-Newtonian fluids, Light WaterTM, FC 600

INTRODUCTION

Between 2000 and 2003, 3M Company phased out the production of Light WaterTM (also called as FC 600) concentrate, AFFF-type formulation designed against fires of polar liquids. During the approximately 30 years of its production, the composition of Light Water concentrate evolved to reflect the progress in the formulation of more effective alcohol-resistant foams, and availability of new and alternate grade ingredients. In total, five types of FC 600 foam formulations were introduced into the market place. The most recent (type 5) entered the market at the beginning of 90s, following the discovery, by Chubb National Foam, that industrial grade xanthan gum in the presence of

polyglycoside surfactants performs equally well as the more expensive Kelco K8A13 xanthan resin¹. Because of this consideration, K8A13 resin (1.2% in type 4 concentrate) was replaced by the industrial grade Keltrol xanthan resin (0.6% in type 5 concentrate) with starch (0.6% in type 5 concentrate) added to adjust the viscosity of the concentrate to correspond approximately to the viscosity of type 4 concentrate.

The pressure-loss and viscosity correlations for 3M Light Water concentrate presented in *3M Light Water Products and Systems Engineering Manual* contained relatively low values of pressure losses and effective viscosity, for given flow rates of the concentrate, as evident in Figures 1 and 2, which present redrawn graphs from the manual². We believe that the data illustrated in Figures 1 and 2 originated in 1970s, corresponding to type 2 or 3 formulation of Light Water concentrate. Subsequently, in 1993, an independent engineering laboratory in Australia performed additional measurements, with the results presented in Figures 3 and 4 as type 4 FC 600³. Recently, the present authors have measured, using a cone and plate viscometer, the apparent viscosity of type 5 FC 600 concentrate as function of temperature, developing power-law and Bulkley-Herschel (i.e., yield pseudoplastic) models of the material. These measurements have then served to develop the effective-viscosity and pressure-loss correlations, which are also illustrated in Figures 3 and 4³.

By comparing Figures 1 and 3, as well as Figures 2 and 4, it is immediately evident that the engineering correlations presented in Figures 1 and 2 differ, respectively, from those illustrated in Figures 3 and 4. As expected, the results for Light Water concentrates of types 4 and 5 display close similarity. This observation leads us to pose three focusing questions for the present study: (i) Are the viscosity measurements presented in Figure 1 internally consistent? (ii) Similarly, are the values of pressure loss presented in Figure 2 internally consistent, and, if so, are they consistent with the measurements illustrated in Figure 1? (iii) Should the measurements included in Figures 1 and 2 be consistent, why do they differ from the data derived from the later experiments, as illustrated in Figures 3 and 4?

The difficulty in comparing the data exhibited in Figures 1-4 is compounded by missing descriptions of the experimental conditions. For example, it is unclear whether the data included in Figure 2 correspond to measurements with multiple pipes or whether the results from experiments with a single pipe were scaled for other pipe diameters. Likewise, it is unclear whether the effective viscosity of Figure 1 was deduced from rheometric measurements or from laminar pipe experiments and then extrapolated to higher flow rates where the turbulent flow exists. Schaefer has recently included in his *ME Thesis* a detailed description of the experiments with type 5 concentrate⁴, but for type 4 even the experimental temperature remains unknown; it is assumed to be 20 °C.

The remainder of this paper is in four parts. The next chapter analyses the effective viscosity data for FC 600 shown in Figure 1. It then compares these data with the two other data sets, outlying their inconsistencies and suggesting corrections. A similar approach is adopted in the following chapter where we dissect the pressure-loss measurements of Figure 2. In the subsequent chapter, we calculate the friction factors from the corrected correlations and compare them with the friction factors deduced from pressure-loss measurements for type 4 concentrate. In the same chapter, we also obtain the pressure-loss predictions from the viscosity model and compare these predictions with the corrected results of Figure 2. The paper concludes with the summary of the major points drawn from the present work.

EFFECTIVE VISCOSITY

The concentrate of FC 600 exhibits time-independent, shear-thinning behaviour. In practical pressure-loss calculations, a small yield stress (in the order of 5 Pa) also displayed by the concentrate can be neglected, with a simple power-law description of the apparent viscosity yielding quite satisfactory predictions³. This means that, the flow curve or rheogram of FC 600 concentrate can be described by Equation 1

$$\tau = m\dot{\gamma}^n \quad (1)$$

where τ denotes the shear stress (in Pa), $\dot{\gamma}$ is the shear rate (in s^{-1}), whereas m (in $Pa\ s^n$) and n (unitless) are called the fluid consistency coefficient and the flow behaviour index. The apparent viscosity is by definition

$$\mu_{app} = \frac{\tau}{\dot{\gamma}} = m\dot{\gamma}^{n-1} \quad (2)$$

For power-law fluids, Equation 2 can be rewritten in terms of the effective viscosity as

$$\mu_{eff} = \frac{\tau_w}{\dot{\gamma}_{nw}} = m'\dot{\gamma}_{nw}^{n'-1} \quad (3)$$

where τ_w denotes the shear rate at the wall that is related to the pressure gradient ($-\Delta P/L$) experienced by a fluid in pipe flow and the internal pipe diameter (D) according to

$$\tau_w = \left(-\frac{\Delta P}{L}\right)\frac{D}{4} \quad (4)$$

In Equations 2 and 3, n , n' as well as m and m' are related as

$$n' = n \text{ and } m' = m\left(\frac{3n+1}{4n}\right)^n \quad (5)$$

Finally, $\dot{\gamma}_{nw}$ is called the nominal shear rate at the wall, corresponding to

$$\dot{\gamma}_{nw} = \frac{32Q}{\pi D^3} = \frac{8V}{D} \quad (6)$$

where Q is the flow rate and V denotes the average velocity. Note the difference between the apparent and effective viscosities. The former is the ratio of shear stress to shear rate for non-Newtonian fluids whereas the latter links pressure losses, $-\Delta P/L$, with the flow rate⁵; i.e. combining Equations 3, 4 and 6 leads to

$$-\frac{\Delta P}{L} = \mu_{eff} \frac{128Q}{\pi D^4} \quad (7)$$

For time-independent fluids, the effective viscosity remains insensitive to pre-shearing history; i.e., μ_{eff} is only a function of $32Q/(\pi D^3)$. Furthermore, for power-law fluids, such as the concentrate of Light Water, the effective viscosity is a unique line, that is straight provided that logarithmic axes are used for ordinate (μ_{eff}) and abscissa ($32Q/(\pi D^3)$). This has been performed in Figure 5, with the result leading us to conclude about the lack of consistency in the original engineering correlation presented in Figure 1.

The data points plotted in Figure 5 fall on separate lines, which are parallel to each other. This may indicate that a single data set, possibly obtained from cone-plate measurements, might have been scaled to yield all results presented in Figure 1 with an algebraic mistake or mistakes made along the way in data processing. For example, if we propose that the scaling involved incorrect calculation of the nominal shear rate at the wall from

$$\dot{\gamma}_{mw} = \frac{32Q}{\pi D^2} \quad (8)$$

rather than from

$$\dot{\gamma}_{mw} = \frac{32Q}{\pi D^3} \quad (6)$$

then all data are drawn to trace a single line, as illustrated by the lower line in Figure 6. Although this correction results in an internally consistent data set, it yields unrealistically low effective viscosity for type 2 or 3 concentrate

$$\text{partially corrected type 2 or 3 concentrate: } \mu_{eff} = 0.385\dot{\gamma}_{nw}^{-0.821} \quad (9)$$

The effective viscosities of the two more recent types of FC 600 concentrates lie significantly higher as recently reported by Dlugogorski et al.³

$$\text{type 4 concentrate: } \mu_{eff} = 11.4\dot{\gamma}_{nw}^{-0.824} \quad (10)$$

$$\text{type 5 concentrate: } \mu_{eff} = 9.11\dot{\gamma}_{nw}^{-0.766} \quad (11)$$

The effective viscosity of Artic Foam 600 from Solberg Scandinavian, a concentrate that has a similar chemical make up to that of FC 600, also exceeds the effective viscosity of Equation 9⁶

$$\text{Arctic Foam 600 concentrate: } \mu_{eff} = 4.11\dot{\gamma}_{nw}^{-0.694} \quad (12)$$

For this reason, we hypothesise that the flow rate was incorrectly converted into GPM, by omitting the factor of 60 owing to conversion between seconds and minutes. Once corrected for this possible omission of the conversion factor, the present data set produces the following equation for the effective viscosity, as illustrated by the upper line in Figure 6

$$\text{corrected type 2 or 3 concentrate: } \mu_{eff} = 11.1 \dot{\gamma}_{nw}^{-0.821} \quad (13)$$

We can now employ Equation 13 to work out more pragmatic engineering correlations for effective viscosity of type 2 or 3 of FC 600 as function of flow rate and internal pipe diameter, as illustrated in Figure 7.

PRESSURE LOSSES

In laminar flow of a power-law fluid, knowledge of the fluid consistency coefficient and the flow behaviour index allows one to calculate immediately the effective viscosity and the pressure losses, for given flow rate and pipe diameter. By replacing for the nominal shear rate at the wall, Equation 7 may also be written as

$$\left(-\frac{\Delta P}{L} \right) \frac{D}{4} = m' \left(\frac{32Q}{\pi D^3} \right)^{n'} \quad (14)$$

With the same assumptions as for the effective viscosity, Equation 14 implies the existence of a unique correlation between the shear stress and the nominal shear rate at the wall. Unfortunately, Figure 8 demonstrates that this does not occur for the data set of Figure 2. However, one observes that the laminar branches are parallel with slopes of around 0.2, consistent with the flow behaviour index ($n' = 0.179$) of the effective viscosity.

It is possible to hypothesise that the discrepancies observed in Figure 8 are a consequence of heat evolution during long pumping experiments or the rheopectic (i.e., viscosity decreasing with time during shearing) nature of the fluid, since the fluid viscosity appears to decrease with increasing pipe diameters. Viscosity of the solution of xanthan-gum concentrates is a weak function of temperature^{3,7}, a phenomenon that would necessitate unrealistically large heating (in the order of 30 °C) during experiments with each consecutive pipe. Similarly, the rheopectic hypothesis needs to be discarded as such behaviour, as opposed to thixotropy, does not seem to occur for solutions of xanthan gum with added starch⁸.

Guided by the fact that the transition from the laminar to turbulent regimes should occur for the same Metzner and Reed Reynolds number, defined as

$$\text{Re}_{MR} = \frac{\rho V D}{\mu_{eff}} = \frac{4 \rho Q}{\mu_{eff} \pi D} = \frac{4 \rho Q}{m' \left(\frac{32Q}{\pi D^3} \right)^{n'-1} \pi D} \quad (15)$$

and from our experience in correcting the effective viscosity we rectify the shear stress values by multiplying them by D and the nominal shear rate by $D^{1/2}$, to obtain the plot presented in the lower part of Figure 9. The reason or reasons of these scaling errors appear unclear, as one would expect the data set of Figure 2 to originate from the direct measurements of pressure gradient by varying the flow rate and pipe diameter. We also realise that there might have been an error in unit conversion and suggest that shear stress values need to be multiply by $165D$, rather than by D , and, similarly, the nominal shear rate by $(165D)^{1/2}$. Unlike, the correction for effective viscosity, where we were able to propose a logical reason for the conversion error, the factor 165 was obtained by ensuring that the

fluid consistency coefficient derived from the laminar pressure loss reflects that deduced from the effective viscosity results of Figure 1, in the least-squares sense. The upper plot in Figure 9 illustrates the result of these computations, with Figure 10 (solid lines) presenting the corrected values of the pressure losses, which correspond to the data of Figure 2.

CALCULATION OF PRESSURE LOSSES FROM VISCOSITY MEASUREMENTS

The corrected values of the shear stress at the wall can be converted to the Fanning friction factor ($\rho = 1300 \text{ kg m}^{-3}$)

$$f = \frac{\tau_w}{\frac{1}{2}\rho V^2} \quad (16)$$

with the results compared in Figure 11 with our earlier calculations for type 4 concentrate³. Detailed appraisal of the figure reveals two differences between these sets of values: Firstly, for the present results, the transition from the laminar to turbulent flow is offset to the Metzner and Reed Reynolds numbers of around 2100 as opposed to 1190 for type 4 concentrate. Secondly, the Blasius equation for the Fanning friction factor applies for Re_{MR} of less than 40,000.

The procedure to calculate the pressure losses from Figure 11 is straightforward, with the results presented as dashed lines in Figure 10.

(i) Select a flow rate and an internal pipe diameter, and then obtain the Metzner and Reed Reynolds number from Equation 15; as an intermediate result, find μ_{eff} from Equation 13 or from Equations 10-12 if pressure losses for other concentrate types are desired.

(ii) Find the Fanning friction factor, using the Re_{MR} of 1190 for transition between laminar and turbulent flows (the value of 2100 may be equally well justified)

$$f = \frac{16}{Re_{MR}} \text{ if } Re_{MR} < 1190; \quad f = \frac{0.0795}{Re_{MR}^{1/4}} \text{ if } 1190 \leq Re_{MR} < 40,000 \quad (17)$$

(iii) Obtain the shear stress at the wall, τ_w , from Equation 16 and then pressure loss, $-\Delta P/L$, from Equation 4.

ACKNOWLEDGEMENTS

The authors acknowledge the support of this work by 3M Company.

CONCLUSIONS

The following points can be drawn from the present investigation:

- One needs to be vigilant when applying the existing engineering correlations for predicting effective viscosity and pressure loss during pumping of foam concentrates, as some data sets are internally inconsistent, and contain erroneous values. Two examples of such correlations were presented in this contribution, together with reasons for the discrepancies and suggestions for the corrections.
- Conversion of engineering correlations between pressure loss and flow rate to a relationship between shear stress at the wall and the nominal shear rate at the wall provide a test for verifying the consistency of pressure-loss correlations. Similarly, engineering correlations for effective viscosity need to be replotted as a function of the nominal shear rate at the wall to verify their internal consistency.
- It is possible to calculate reliably the effective viscosity and pressure losses during pumping of xanthan-based foam concentrates as function of flow rate and internal pipe diameter. The calculation procedure necessitates the knowledge of the apparent viscosity of the concentrate, from rheometric measurements, and makes the use of the Blasius equation for friction factor in the turbulent regime. The transition from laminar to turbulent flow for xanthan-based concentrates appears to occur over a range of Metzner and Reed Reynolds numbers of between 1190 and 2100.

REFERENCES

- [1] Norman E.C and A.C. Regina (1991) *Alcohol Resistant Aqueous Film Forming Foam*, US Patent 4,999,119.
- [2] *3M Light Water Products and Systems Engineering Manual* (1991), Fire Protection Systems, 3M Industrial Chemical Products Division, St. Paul MN, USA.
- [3] Dlugogorski B.Z., Schaefer T.H. and E.M. Kennedy (2005), “Friction factors for pipe flow of xanthan-based concentrates of fire-fighting foams”, accepted for presentation at the 8th *International Symposium on Fire Safety Science*, Beijing, September 2005.
- [4] Schaefer T.H. (2005) *ME Thesis*, The University of Newcastle, Australia.
- [5] Chhabra R.P. and J.F. Richardson (1999) *Non-Newtonian Flow in the Process Industries: Fundamentals and Engineering Applications*, Butterworth-Heinemann, Oxford.
- [6] Jacobs L. (2005) *Pressure Drop and Apparent Viscosity Calculations*, Personal Communication.
- [7] Marcotte M., Hoshahili A.R.T. and H.S. Ramaswamy (2001) “Rheological properties of selected hydrocolloids as a function of concentration and temperature” *Food Research International* **34**, 695-703.
- [8] Korus J., Juszczak L., Witczak M. and B. Achremowicz (2004) *International Journal of Food Science and Technology* **39**, 641-652.

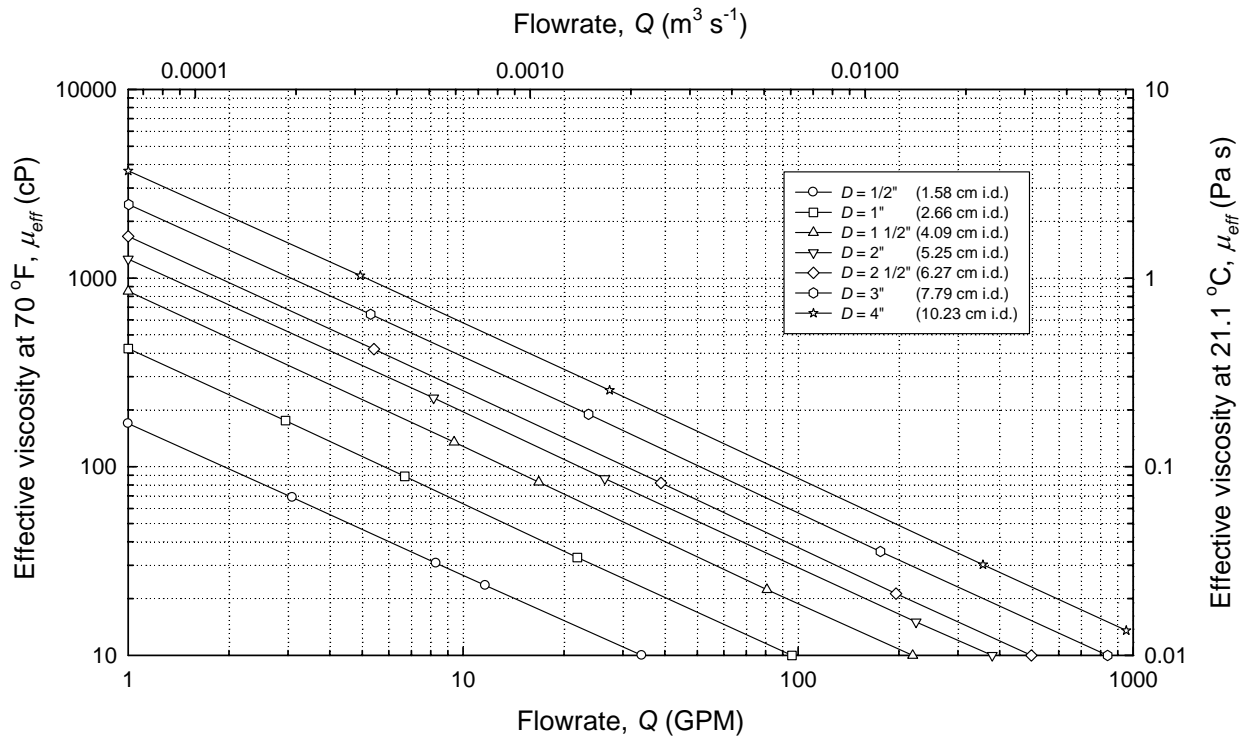


Figure 1. Variation of the effective viscosity with flow rate and pipe diameter, replotted from *3M Light Water Products and Systems Engineering Manual*². All measurements in the figures are for Schedule 40 pipes. The points were added to identify the solid lines.

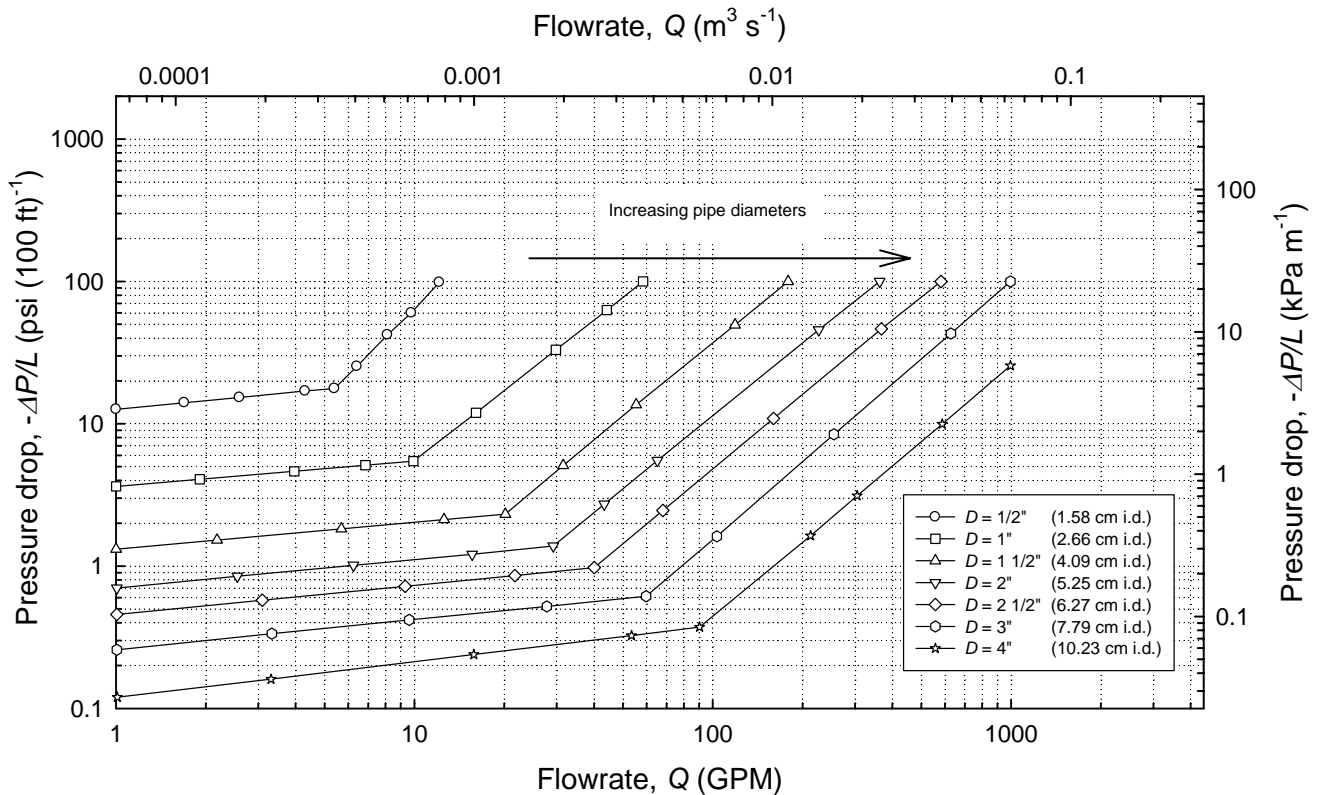


Figure 2. The effect of flow rate and pipe diameter on the pressure loss during pumping of FC 600 concentrate, replotted from *3M Light Water Products and Systems Engineering Manual*². The points were added for convenience to identify the solid lines.

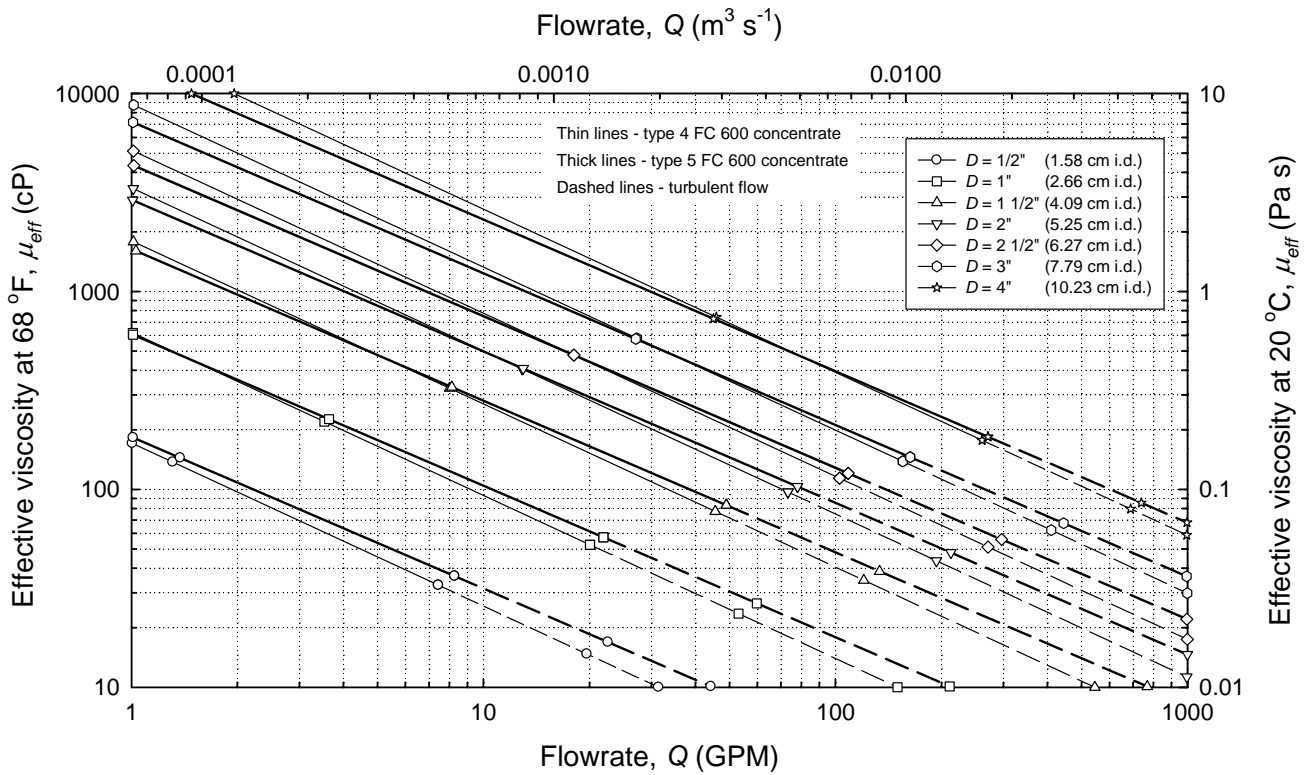


Figure 3. The effective viscosity exhibited by types 4 and 5 Light Water concentrate. The data for type 4 were deduced from the pressure-loss experiments and those for type 5 from the apparent viscosity measured with a cone and plate rheometer³. Points identify the trends.

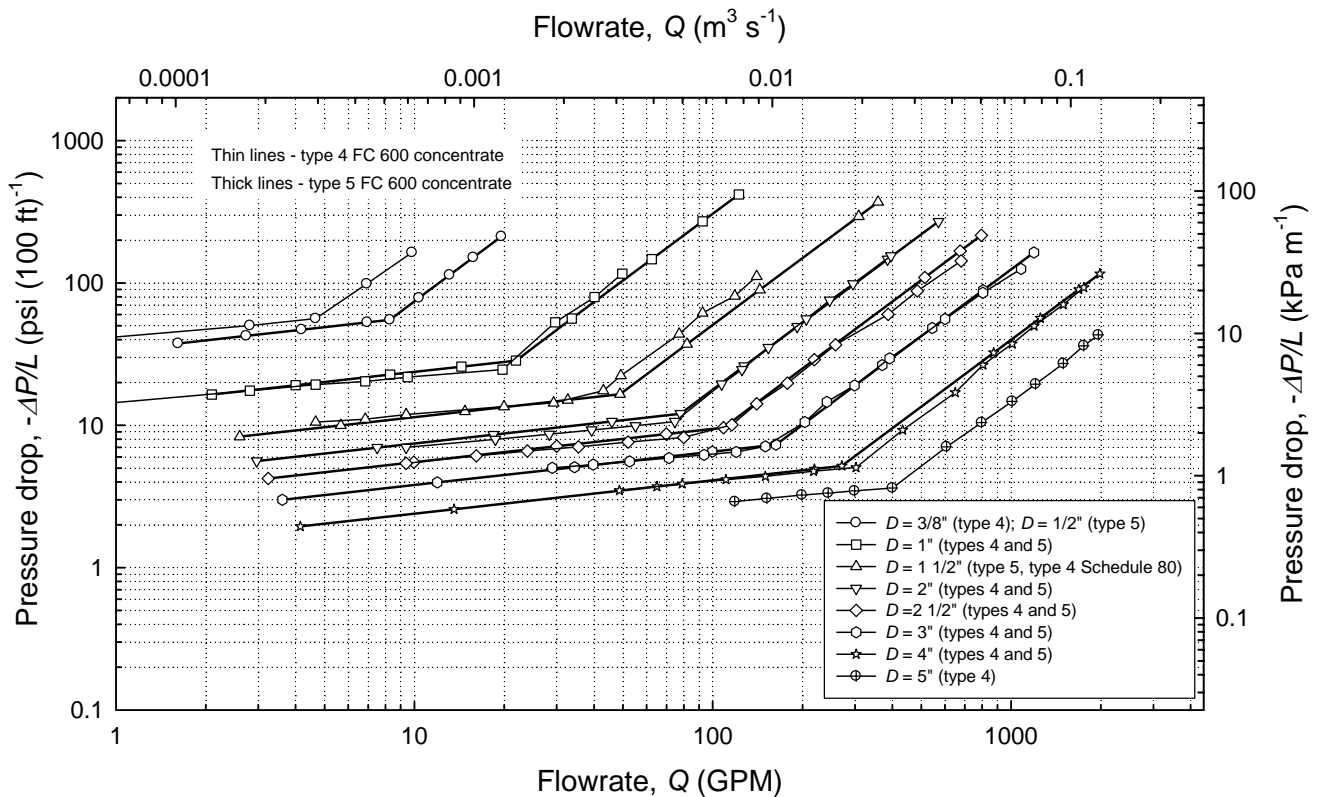


Figure 4. Pressure losses for type 4 (from direct measurements) and type 5 (deduced from the apparent viscosity and the Blasius equation) concentrates³. Points identify the trends.

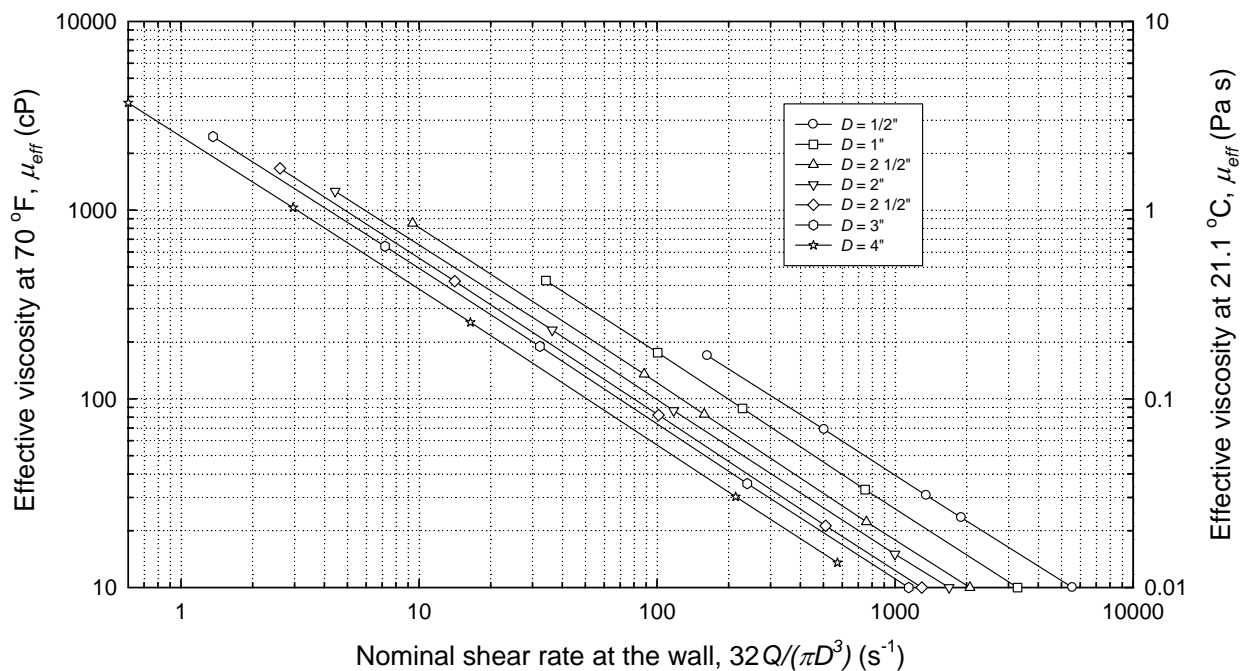


Figure 5. The relationship between the effective viscosity and the nominal shear rate at the wall, for the data set illustrated in Figure 1.

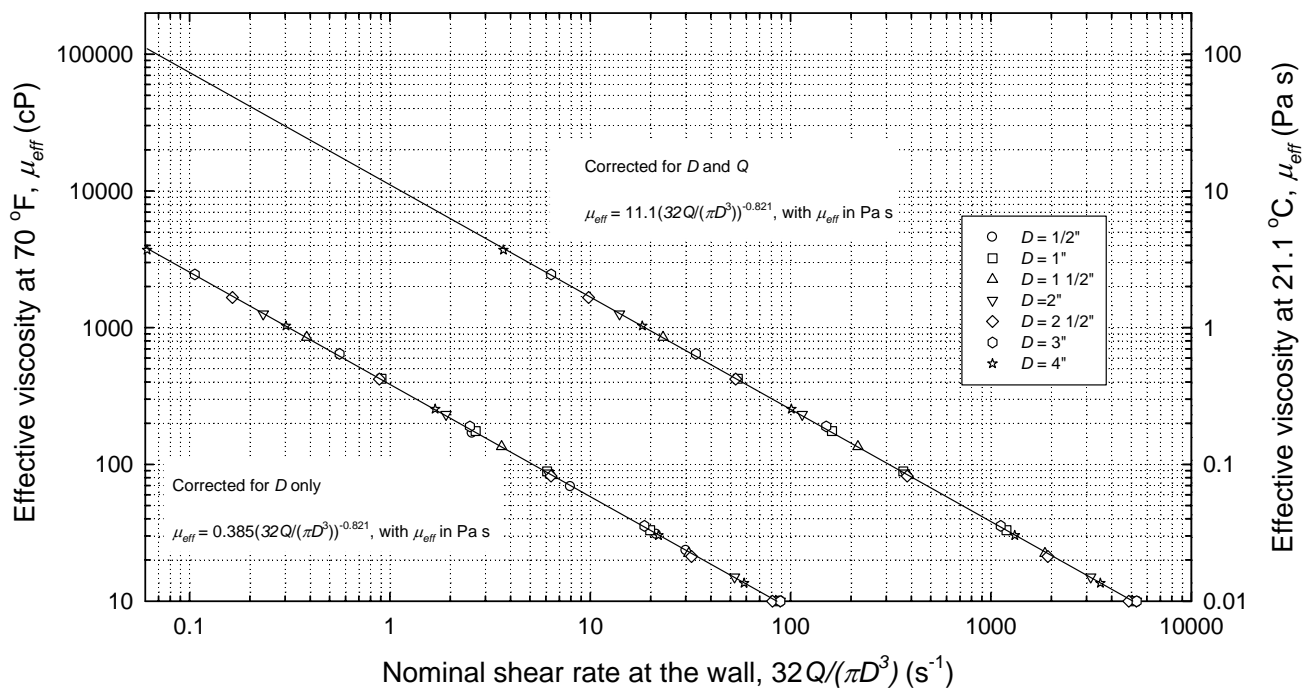


Figure 6. Two attempts to correct the inconsistencies in the effective-viscosity results, as highlighted in Figure 5. The original data have been taken from Figure 1.

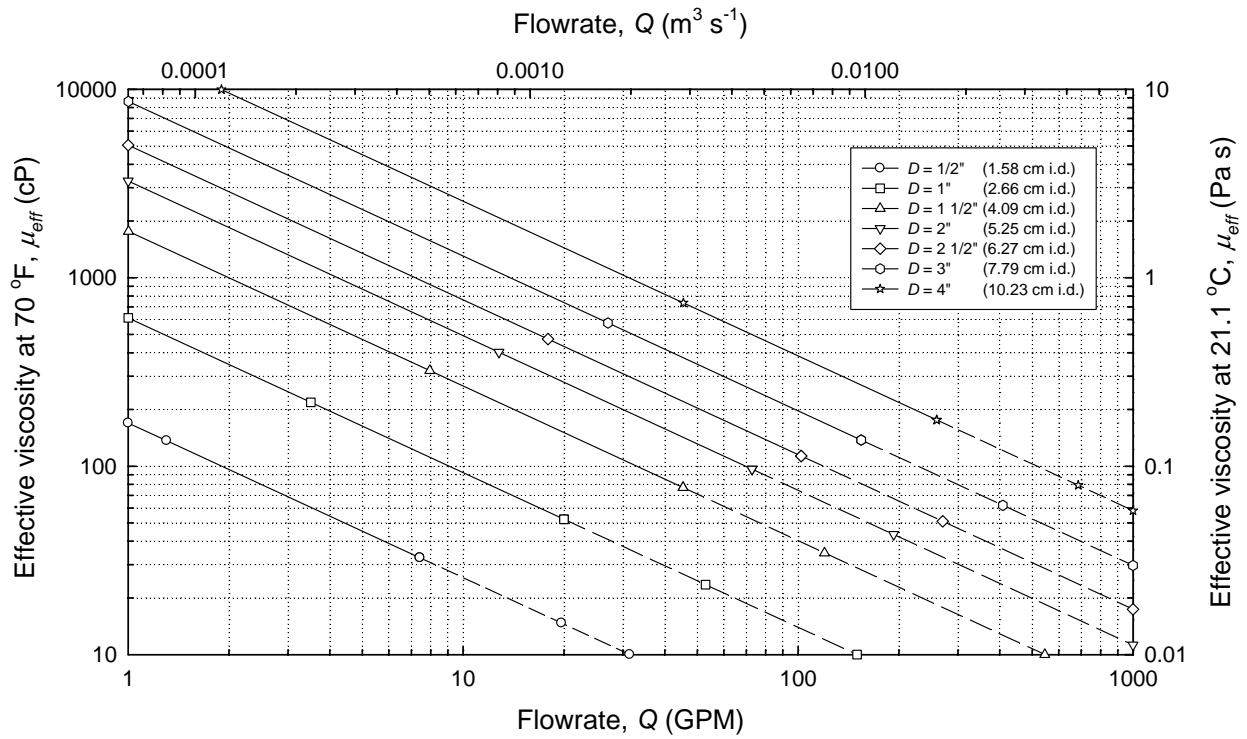


Figure 7. Internally-consistent engineering correlations for the effective viscosity of FC 600, corresponding to the values presented in Figure 1. Dashed lines reflect turbulent regime.

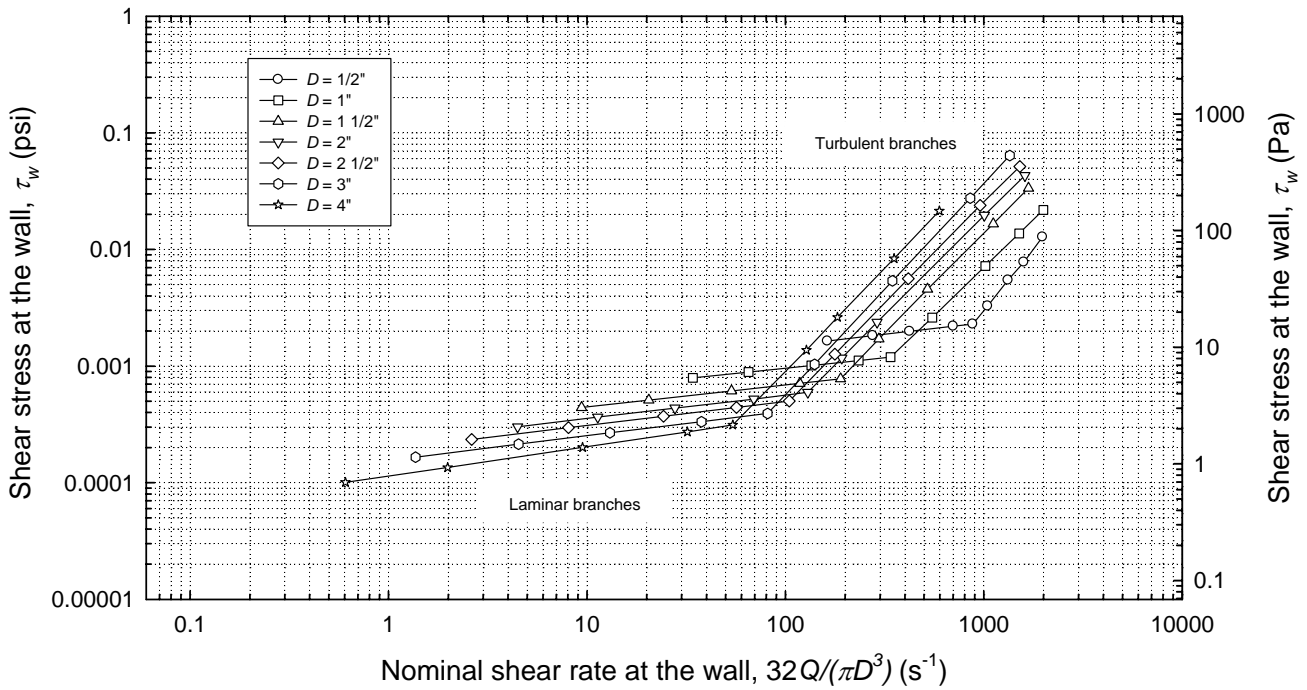


Figure 8. The relationship between the shear stress and the nominal shear rate at the wall, as derived from the data set illustrated in Figure 2.

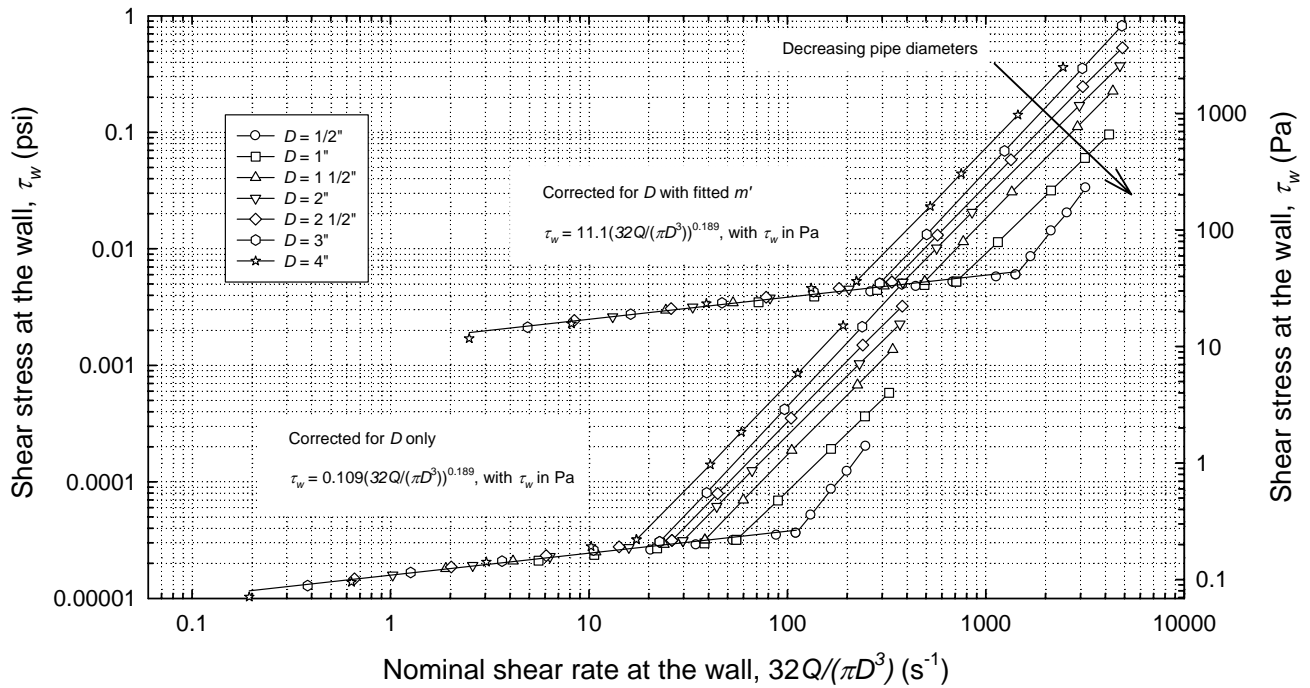


Figure 9. Two attempts to correct the inconsistencies in the pressure-loss data, as highlighted in Figure 8. The original data have been taken from Figure 2.

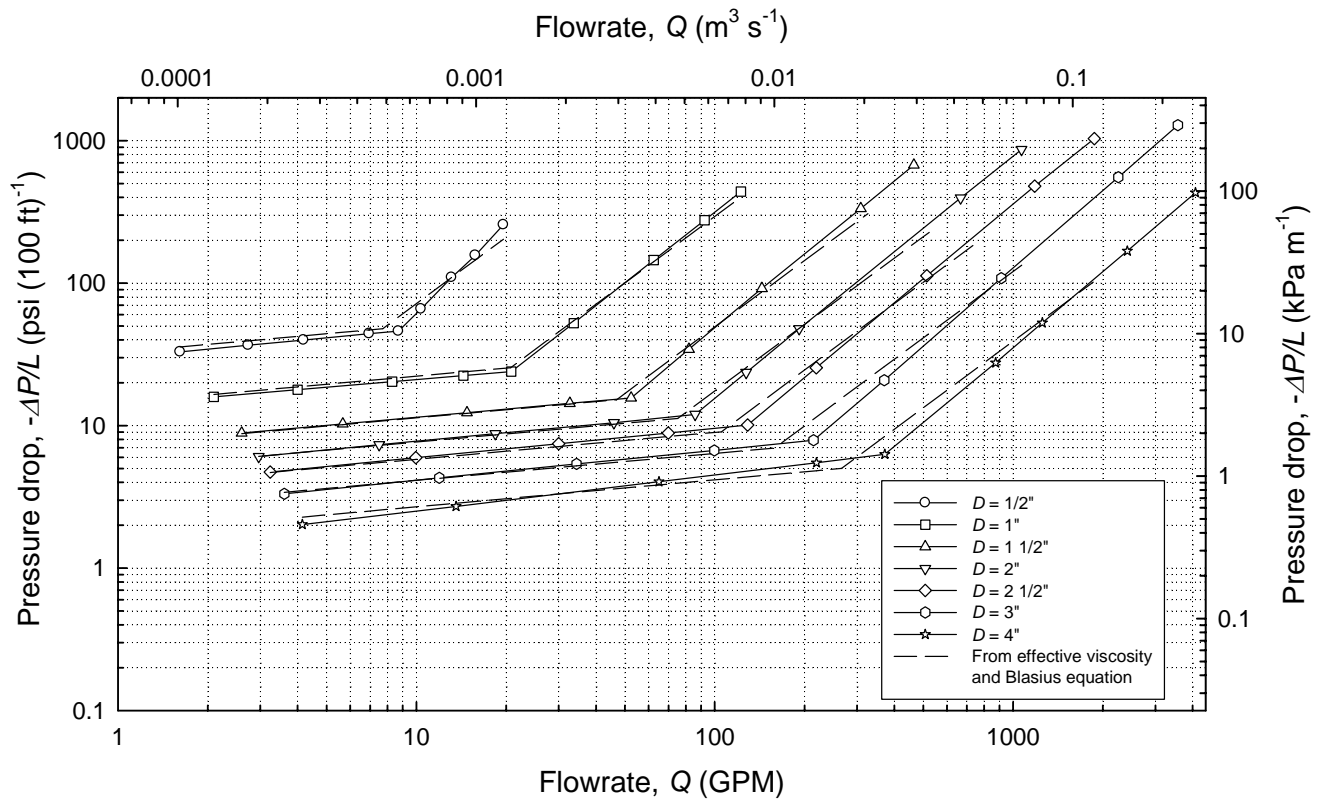


Figure 10. Internally-consistent engineering correlations for the pressure loss of FC 600 formulation during pumping of the concentrate in smooth pipes. The solid lines correspond to the corrected data initially illustrated in Figure 2. The dashed lines follow from the corrected effective-viscosity data, initially introduced in Figure 1, by assuming the transition to

turbulent flow to occur at the Metzner and Reed Reynolds number of 1190 and using the Blasius equation for the Reynolds numbers of up to 40,000³.

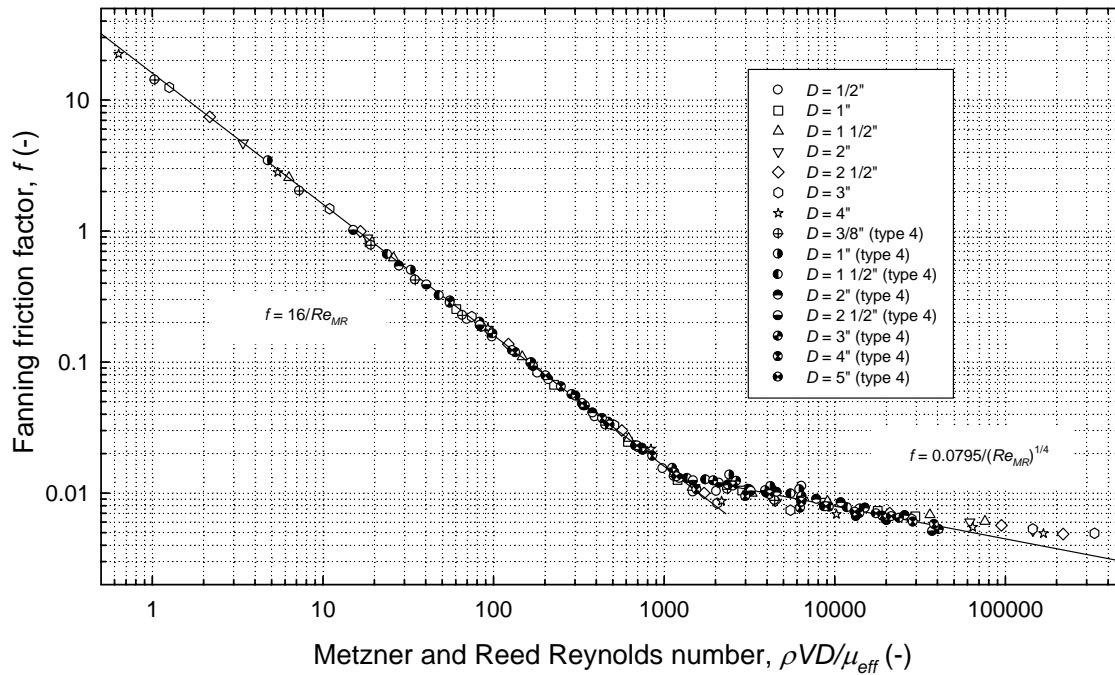


Figure 11. Friction factor plot for FC 600 concentrate. Open symbols correspond to the corrected data derived from *3M Light Water Products and Systems Engineering Manual*². The points denoted as type 4 were derived from the experimental measurements obtained in Australia in 1993³.